International Journal of Innovation in
Mechanical Engineering and Advanced Materials
Vol. 7 (No. 2), 2025, pp. 74-87
Journal homepage: publikasi.mercubuana.ac.id/index.php/ijimeam
DOI: 10.22441/ijimeam.v7i2.31555

Numerical Analysis of Heat Transfer Enhancement in Wavy Trapezoidal and Rectangular Microchannels

Soumik Kumar Hazra *

Department of Mechatronics Engineering, Faculty of Engineering, University of Debrecen, Otemeto Utca 2-4, Debrecen 4028, Hungary
*Corresponding Author: soumikhazra4390@mailbox.unideb.hu (SKH)

Abstract

This study presents a comprehensive Computational Fluid Dynamics (CFD) analysis of heat transfer enhancement in microchannels with varying geometries, specifically focusing on wavy microchannels with trapezoidal and rectangular cross-sections. Water is used as the working fluid, and silicon is selected as the solid wall material. A three-dimensional conjugate heat transfer model is developed by solving the steady-state Navier–Stokes and energy equations using the finite volume method in ANSYS Fluent, with the SIMPLEC algorithm employed for pressure–velocity coupling. The analysis examines the influence of cross-sectional shape and wall waviness on thermal performance, while maintaining a constant hydraulic diameter across all configurations. Eight different geometries, including straight and wavy versions of rectangular and trapezoidal cross-sections with varying top-to-bottom width ratios (0.075–0.055 mm), are evaluated over a Reynolds number range corresponding to inlet velocities of 0.5–4.0 m/s. Results show that wavy microchannels significantly enhance heat transfer compared to their straight counterparts. For instance, at 4 m/s, the Nusselt number for the wavy rectangular microchannel reaches 9.48, compared to 7.19 for the straight rectangular configuration, representing a 32% enhancement. Similarly, the wavy trapezoidal channel with a top width of 0.18 mm achieves a maximum Nusselt number of 9.25, compared to 7.19 for its straight equivalent, indicating a 29% improvement. Additionally, the Nu/Nu_0 versus Re plots reveal a consistent trend of increased heat transfer due to wall waviness across all geometries, with negligible influence from cross-sectional shape when hydraulic diameter is kept constant. The study demonstrates that incorporating wavy structures into microchannel designs significantly improves thermal performance with minimal increases in pressure drop, and that the effect is driven more by wall geometry than by cross-sectional shape. These findings provide valuable insights for the development of compact and efficient microchannel heat sinks for electronic cooling applications.

Article Info:
Received: 2 January 2025
Revised: 6 April 2025
Accepted: 9 April 2025
Available online: 14 April 2025

Keywords:
Microchannel Heat Sink (MCHS); wavy microchannels; heat transfer enhancement; Nusselt number; Computational Fluid Dynamics (CFD)

How to cite:

S. K. Hazra, "Numerical analysis of heat transfer enhancement in wavy trapezoidal and rectangular microchannels," *Int. J. Innov. Mech. Eng. Adv. Mater*, vol. 7, no. 2, pp. 74-87, 2025

1. Introduction

The current trend of miniaturization of electronic packages and increase in power density are the main reasons why traditional cooling approaches using fans are becoming impractical or unable to meet the increasing cooling demands of electronic devices. The critical bottleneck for the development of technically advanced electronic products is thermal issues [1]. According to the report published by the International Technology Roadmap for Semiconductors (ITRS), the reason behind peak power consumption was the ongoing COVID-19 pandemic when most people were forced to work from home due to safety reasons, and that boosted the sales of PCs by 11% in 2020. Overall growth of semiconductors is expected to continue in 2021 at a rate of 5% to 7%, which will raise the power consumption by 96% (147 W–288 W) in 2022 [2]. These developments underscore the urgent need for more efficient cooling technologies to maintain device reliability and performance under escalating thermal loads.

Recent advancements in microfabrication technology have facilitated the development of microchannel heat sinks (MCHS) with complex and efficient designs, surpassing the limitations of conventional straight, featureless microchannels [3]. An experimental study by Tuckerman and Pease demonstrated the effectiveness of rectangular microchannels in cooling VLSI chips, achieving a heat removal rate of 790 W/cm^2 using water as the coolant [4]. This high cooling capacity was primarily

attributed to the increased surface area-to-volume ratio of the microchannels. The success of this approach laid the foundation for further applications in electronics and laser-based thermal management systems.

Deionized water remains a preferred coolant due to its affordability, availability, and stability. To maintain safe operation, the temperature of electronic devices must remain below water's boiling point, ensuring single-phase liquid flow. Over the years, three-dimensional Navier–Stokes-based models incorporating conjugate heat transfer have been widely employed in MCHS simulations. Earlier research explored the effects of various design parameters, including channel dimensions, surface roughness, boundary conditions, and temperature-dependent fluid properties [5]–[7]. Close agreement between experimental and numerical results has been achieved due to significant improvements in measurement techniques and computational accuracy over the past three decades [8].

Studies have shown that the influence of relative surface roughness below 10^{-5} is negligible. Additionally, accounting for temperature-dependent fluid properties is essential in numerical modeling. For instance, conjugate heat transfer simulations have indicated up to an 11.7% increase in thermal performance when including a 250 μm thick bottom wall, and up to 20% improvement when replacing silicon with copper as the wall material—primarily due to enhanced axial and vertical heat conduction [3]. Importantly, when microchannel walls are straight and featureless, the thermal boundary layer thickens progressively along the flow direction, thereby impeding effective heat transfer.

An effective approach to addressing the thermal limitations of high-performance electronics is direct liquid cooling using MCHS [9], [10]. Research in this domain has explored both single-phase and two-phase (boiling) cooling methods. Although two-phase cooling offers significantly higher heat removal capabilities, it also introduces complex phenomena such as condensation, critical heat flux, nucleation dynamics, and saturation temperature control, making it more challenging to implement reliably in practical systems [3]. The pioneering work of Tuckerman and Pease sparked considerable interest in microchannel-based thermal management, establishing the foundation for subsequent innovations in microchannel design.

Among the key design variables influencing microchannel performance are channel geometry, surface features, and material properties [11]. Conventional MCHSs often utilize straight channels, which limit thermal performance due to nearly unidirectional flow paths, resulting in inefficient convective heat transfer and poor fluid mixing. This leads to temperature non-uniformity across the integrated circuit (IC) surface, the formation of thermal hotspots, and thickening of the thermal boundary layer along the flow directional which degrades cooling efficiency and device reliability. Such thermal gradients can accelerate material fatigue and contribute to premature failure in high-density electronics.

To overcome these limitations, researchers have proposed modifications to microchannel designs, including the use of geometrical enhancements such as wavy walls, reentrant cavities, and semi-octagonal or trapezoidal cross-sections [12]–[15]. These structures promote secondary flow and disruption of boundary layers, leading to improved convective heat transfer. However, such improvements often come at the cost of increased pressure drop and higher pumping power requirements, which may hinder the feasibility of implementation in real-world applications.

Therefore, an optimal microchannel design must strike a balance between enhanced thermal performance and acceptable hydraulic resistance. Recent numerical investigations have demonstrated that it is possible to achieve significant heat transfer enhancement while maintaining manageable pressure drops through intelligent geometric optimization [16]–[18]. This balance is crucial for ensuring both thermal efficiency and system-level energy sustainability in next-generation electronic cooling systems.

Despite significant progress in the development of MCHS designs, a fundamental challenge remains enhancing heat transfer performance without inducing excessive pressure drop or increasing manufacturing complexity. While numerous studies have examined the effects of cross-sectional variations and surface features, relatively little attention has been paid to the combined influence of wall waviness and trapezoidal geometries, particularly under the constraint of a fixed hydraulic diameter. This study addresses this research gap by systematically evaluating and comparing the thermal performance of wavy and straight microchannels with both rectangular and trapezoidal cross-sections.

The primary objective of this work is to investigate numerically how different channel geometries—specifically simple (straight) and wavy profiles, affect heat transfer behavior while maintaining consistent boundary conditions and hydraulic diameter using Computational Fluid Dynamics (CFD)

analysis. Both rectangular and trapezoidal microchannels with varying dimensions are analyzed in detail. Through a comprehensive parametric study, the configurations that yield optimal thermal performance are identified. A key contribution of this research lies in isolating the effect of shape-induced flow disturbances on thermal enhancement, thereby offering valuable insights into the physics of flow structures within these channels. The findings emphasize the importance of geometric optimization in advancing the design of efficient and compact thermal management systems for high-performance electronic applications.

2. Methods

In this study, eight microchannel configurations with varying shapes, dimensions, and properties were investigated to evaluate the effects of geometry on heat transfer enhancement. The analysis focused on both rectangular and trapezoidal microchannels, comparing simple (straight) and wavy forms. Specific attention was given to the influence of hydraulic diameter and the aspect ratio of trapezoidal channels, all under the condition of constant hydraulic diameter, to facilitate a fair comparison of thermal performance.

Numerical simulations were performed using the commercial Computational Fluid Dynamics (CFD) software ANSYS Fluent 16. The steady-state, incompressible Navier–Stokes equations were solved using Reynolds Stress Model (RSM). Pressure-velocity coupling was handled via the SIMPLE algorithm, with standard pressure discretization applied. Second-order upwind schemes were used for both momentum and energy equations to ensure higher accuracy. Thermal boundary conditions were directly implemented in Fluent, including a uniform heat flux at the bottom surface of the silicon substrate (1,000,000 W/m^2) and an adiabatic condition at the top surface. Periodic boundary conditions were applied to the lateral sides of the computational domain.

To represent realistic thermal and flow conditions, a uniform inlet velocity profile was prescribed, while an outflow condition was applied at the outlet. No-slip boundary conditions were imposed on all solid walls. The working fluid, liquid water, entered the channel at a temperature of 293 K, and the inlet wall was maintained at the same temperature. Convergence criteria for the continuity and energy equations were set at 1×10^{-6} and 1×10^{-8}, respectively, ensuring numerical stability and accuracy.

To simplify the analysis, several standard assumptions were adopted:

- Steady-state and laminar flow conditions
- Newtonian and incompressible fluid behavior
- Negligible viscous dissipation
- Constant thermophysical properties, with piecewise linear variations of thermal conductivity and viscosity with temperature [20]
- Negligible radiative and natural convective heat transfer
- Neglect of Electrical Double Layer (EDL) effects, justified by the hydraulic diameters being well above 40 μm, where EDL influence is minimal [21]

These assumptions are consistent with those commonly employed in microchannel heat transfer studies and provide a reliable framework for modeling the behavior of silicon-based MCHS cooled by water.

All relevant variables and terms used in the mathematical formulations are detailed in the Nomenclature section.

2.1. Geometry and domain description

The geometries used in this study for numerical simulation include both rectangular and trapezoidal microchannels, in simple (straight) and wavy configurations. Figure 1(a) illustrates a straight rectangular microchannel made of silicon, subjected to a uniform heat flux at the bottom wall. Water is used as the working fluid. The computational domain for this configuration has a total length (L) of 10 mm, width (W) of 0.3 mm, and height (H) of 0.35 mm. The microchannel itself has a width (W_c) of 0.1 mm and a height (H_c) of 0.2 mm, resulting in a hydraulic diameter (D) of 133 μm.

Figure 1(b) shows the wavy rectangular microchannel with the same domain dimensions as the straight rectangular channel. It incorporates four full sinusoidal waves along the flow direction, each with an amplitude (A) of 2.5 mm. The cross-sectional dimensions and hydraulic diameter remain identical to the straight rectangular channel, allowing for a direct comparison of flow and thermal performance.

Figures 2 through 4 present the geometries of trapezoidal microchannels—both straight and wavy—designed by varying key dimensional parameters. Each configuration maintains a domain

length of 10 mm, height of 0.35 mm, and width of 0.3 mm, with a wave amplitude of 2.5 mm in the wavy cases.

- Figure 2(a–b): The first trapezoidal configuration features a base width (W_{cb}) of 0.075 mm, a top width (W_{ct}) of 0.125 mm, and a channel height (H_c) of 0.2 mm. Both the straight and wavy variants of this geometry share a hydraulic diameter of 133 μm.
- Figure 3(a–b): The second trapezoidal design narrows the base width to 0.055 mm and increases the top width to 0.15 mm, keeping the channel height at 0.2 mm. These also maintain a hydraulic diameter of 133 μm.
- Figure 4(a–b): The third configuration retains the base width at 0.055 mm but extends the top width to 0.18 mm, resulting in a slightly larger hydraulic diameter of 144 μm. The channel height remains at 0.2 mm.

The wavy walls are mathematically described by the equation $y = A\cos(2\pi x/L)$, where A is the wave amplitude and L is the wavelength. For computational efficiency, the domain used in simulations consists of 10 to 12 full wavy cycles, ensuring sufficient periodicity for thermal and hydrodynamic analysis. To reduce computational cost while maintaining accuracy, symmetry conditions in the x–y plane were utilized, allowing simulations to be performed on half of the geometry under constant wall temperature and heat flux conditions. In all configurations, silicon was used as the solid wall material due to its high thermal diffusivity, which ensures relatively uniform heat distribution across the substrate during conjugate heat transfer simulations.

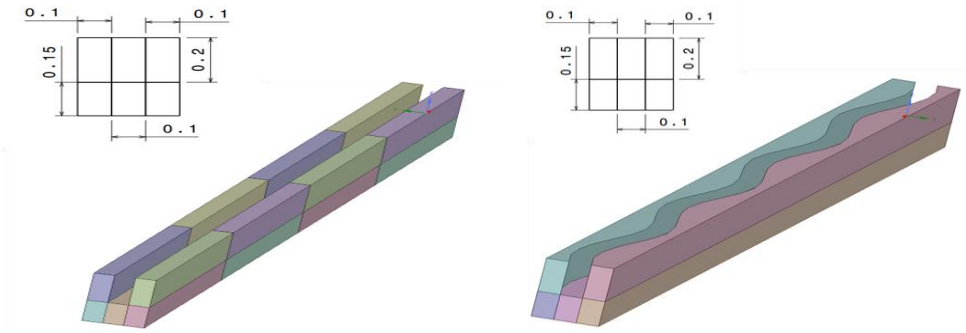

(a) (b)

Figure 1. Rectangular microchannel, (a) Straight (b) Wavy

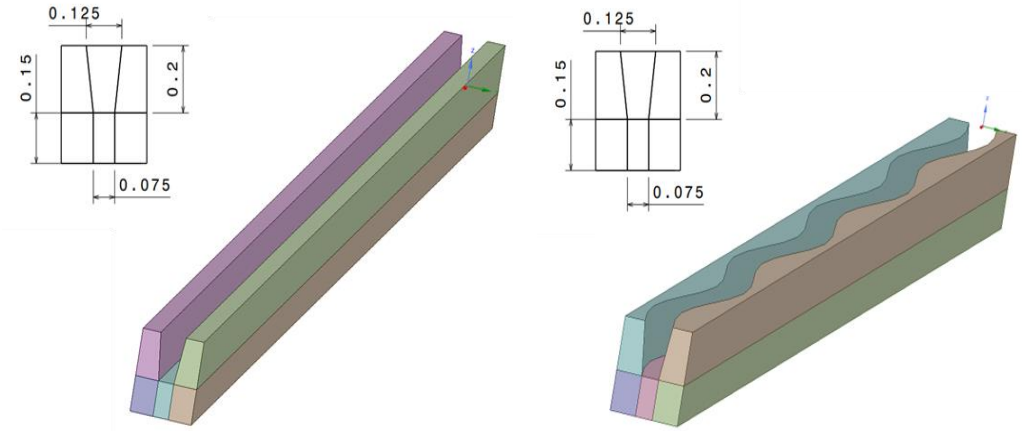

(a) (b)

Figure 2. Trapezoidal (0.075 mm base) channel, (a) Straight (b) Wavy

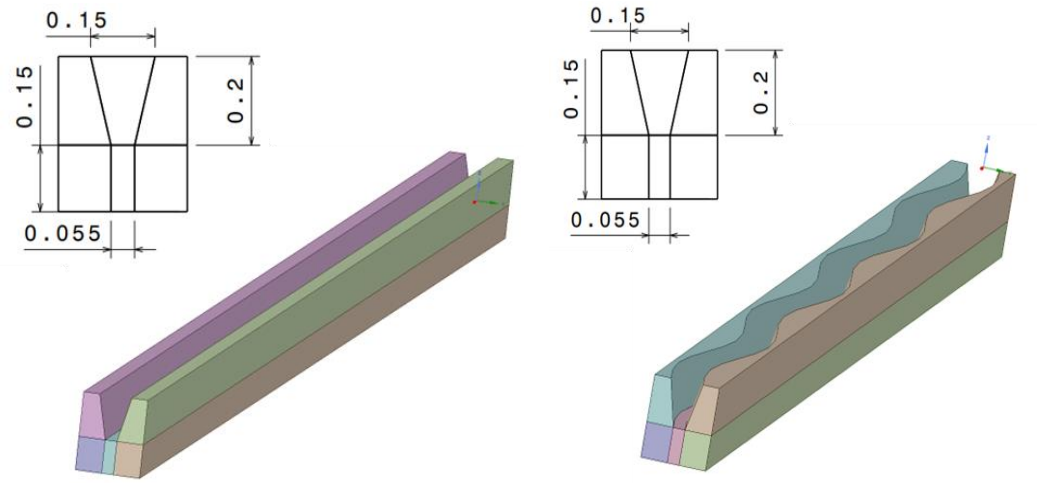

(a) (b)

Figure 3. Trapezoidal (0.055 mm base) channel, (a) Straight (b) Wavy

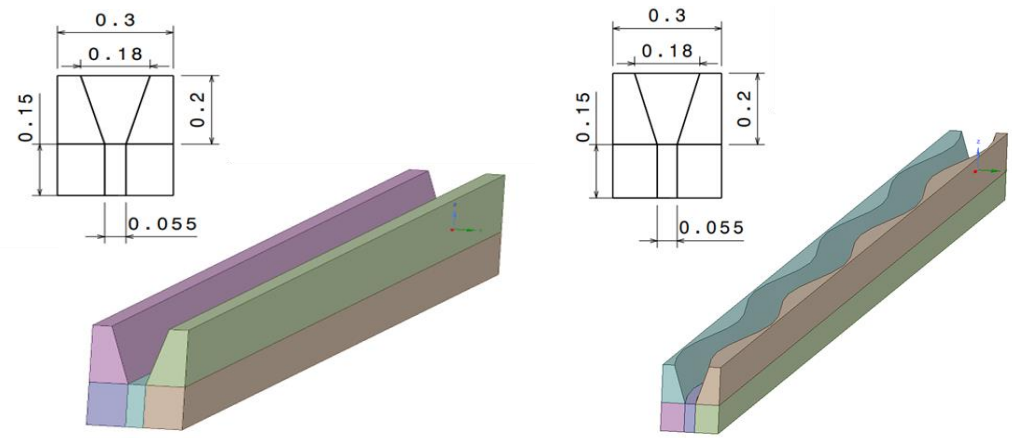

(a) (b)

Figure 4. Trapezoidal (0.18 mm top) channel, (a) Straight (b) Wavy

2.2. Numerical formulation

The governing equations for the conservation of mass, momentum, and energy in the liquid phase, along with the energy equation for the solid domain, are expressed below.
The continuity equation is given by

$$\nabla \cdot (\rho\, \bar{u}) = 0 \tag{1}$$

Conservation of momentum is described by

$$\rho(\bar{u} \cdot \nabla \bar{u}) = -\nabla p + \mu\, \nabla^2 \cdot \bar{u} + \bar{F} \tag{2}$$

Energy for the liquid

$$\rho c_p \left(\bar{u} \cdot \nabla T_f\right) = k_f\, \nabla^2 T_f \tag{3}$$

In solid regions, the energy transport equation has the following form:

$$\nabla \cdot (\bar{u} \rho h) = \nabla \cdot (k \nabla T) + S \tag{4}$$

The applied boundary conditions are

- At the inlet side (x = 0), a uniform velocity profile was imposed with components (u = u_{in}, v = w = 0) and temperature (T= 293 K) has been applied.

- At the outlet side (x = L), the fluid pressure and temperature are specified as $p|_{x=L} = pout = 0$ and $(\partial T/\partial x)|x=L = 0$ [22].
- For the solid wall at the inlet and exit sides (at x = 0 and x= L) , insulated condition is given by $\partial Ts/\partial x = 0$, following the existing practice [23],[24].
- The top surface (z = H) of a heat sink is assumed to be covered by Pyrex plate. So, insulated heat transfer conditions are adopted by $(\partial Ts/\partial z)|_{z=H}=0$ as a reasonable assumption.
- At the bottom wall (z = 0), constant heat flux (106 W/m2) is given by $-ks(\partial Ts/\partial z) = q = 106$ W/m^2.
- At the fluid–solid interface, no slip condition, no penetration and equal temperature are given as $u = v = w = 0$ and $T_s = T_f$.
- At the two opposite sides of the channel (y = 0 and y = W), the symmetrical conditions are given by $\partial T/\partial y = 0$, $\partial u/\partial y = 0$, and v = w = 0 due to periodicity.
- Total bottom area of the channel = 0.3 x L_c.
- Total Heat transfer (Q) = 1,000,000 $\mathrm{watt/m^2}$ x Bottom wall area

Reynolds number is calculated by the velocity of fluid u_{in}, hydraulic diameter D_h as

$$Re = (\varrho_{f,\,in} D_h u_m) / \mu_{f,avg} \tag{5}$$

Hydraulic mean diameter and weighted area of the channel are calculated by following equations:

$$D = \frac{2 \times (Wc \times Hc)}{(Wc + Hc)} \tag{6}$$

$$W = \frac{Wc \times Lc}{2(Hc \times Lc)} \tag{7}$$

Convective Heat transfer coefficient, Nusselt Number, and Friction factor are calculated by:

$$h = \frac{Q}{(weighted\ area \times (Tw - Tf))} \tag{8}$$

$$Nu = \frac{(D \times h)}{(K_{water\ at\ Tf})} \tag{9}$$

$$f = \frac{(2 \times (P_{inlet} - P_{outlet}) \times D)}{(\varrho_f \times (u_{in})^2 \times L)} \tag{10}$$

2.3. Grid independency test

A grid independency test was conducted to determine an appropriate mesh size that ensures accurate and reliable simulation results. We have compared the mesh with 800,000 grids and 1,200,000 grids and observed that there is no significant change in results between these two mesh. The results obtain the relative error in Nusselt number and friction factor at different grid numbers for wavy trapezoidal microchannel for inlet velocity of 2 m/sec. The percentage error is calculated by differentiating m_1 from m_2 and by doing percentage calculation upon m_1 where m represents any parameter such as Nusselt number and friction factor, m_1 represents finest grids and m_2 represents coarse grids. From the analysis it is evident that 800,000 grids are enough for our further calculations.

3. Results and Discussion

This study investigates the enhancement of heat transfer in trapezoidal microchannels through the introduction of sinusoidal wall undulations. Four distinct cross-sectional geometries were analyzed: one rectangular and three trapezoidal configurations with varying dimensions, to assess the impact of geometric modifications on thermal performance. Details of the waveform geometry are provided in the geometry description section. All simulations were conducted assuming silicon as the channel wall material, with a constant specific heat capacity of 702 J/kg·K and thermal conductivity of 148 W/m·K. Water was used as the coolant. The inlet velocity of the coolant was varied between 0.5 m/s and 4 m/s to study the influence of the Reynolds number (Re) on heat transfer

behavior. The Nusselt number (Nu) was used as the primary parameter to evaluate heat transfer efficiency, where higher Nu values indicate improved thermal performance. Additionally, the study examined the effect of hydraulic diameter by including a configuration with a distinct channel size. Numerical simulations were carried out using ANSYS Fluent 16.0 to obtain bottom wall temperatures, coolant outlet temperatures, and pressure values at the inlet and outlet. These data were subsequently used to calculate the Nusselt number and analyze the thermal performance of each geometry. The following subsections present a detailed discussion of the heat transfer enhancements observed across the various microchannel configurations.

3.1. Rectangular cross-section

Initially, a rectangular microchannel with a hydraulic diameter of 0.133 mm, was analyzed. Simulations of the straight channel configuration revealed a direct correlation between Reynolds number and heat transfer, with increasing Re leading to enhanced heat transfer. Concurrently, pressure drop across the channel increased, while the friction factor decreased. Upon transitioning from a straight to a wavy channel geometry, a more pronounced increase in Nusselt number with increasing Re was observed, as illustrated in Figure 5. This indicates that the heat transfer enhancement becomes more significant at higher inlet water velocities which are tabulated below in table 1 and 2. Also Nu/Nu_0 against Re graph has been plotted to validate the heat transfer enhancement (Figure 6).

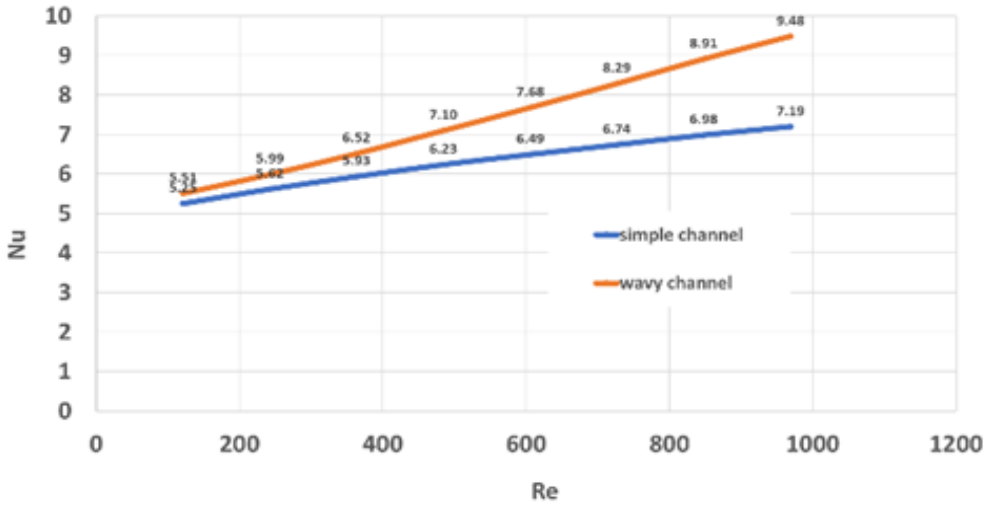

Figure 5. Comparison of Nusselt number in wavy and straight rectangular channel versus Reynold number

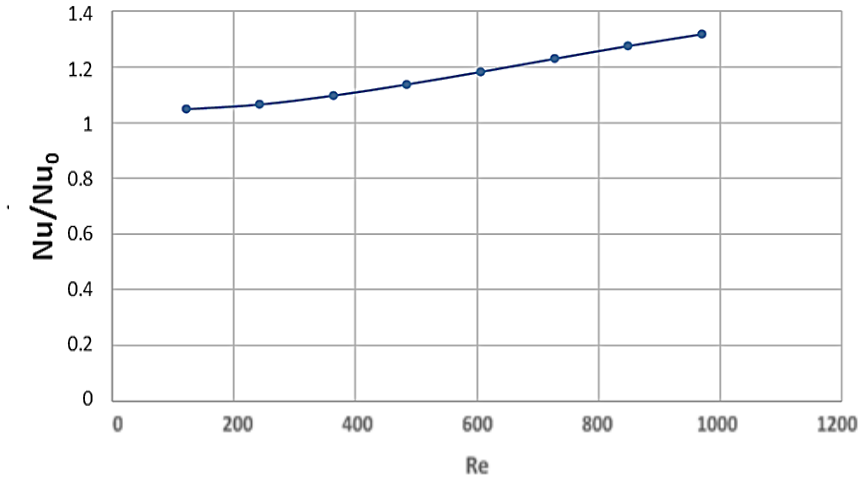

Figure 6. Comparison of Nu/Nu_0 versus Re for rectangular channel

Table 1. Results of straight rectangular microchannel simulation

Inlet Velocity (m/s)	T_w (K)	T_f (K)	P_{inlet}	P_{outlet}	h at T_f	Nu	Friction factor (f)
0.5	346.94	323.43	4706.99	170.60	25521.24	5.25	0.485
1	331.10	308.39	11846.75	659.78	26411.55	5.62	0.299
1.5	325.17	303.36	20019.09	1470.40	27504.84	5.93	0.220
2	321.79	300.83	28980.30	2600.15	28617.99	6.23	0.176
2.5	319.50	299.30	38630.93	4048.71	29693.71	6.49	0.148
3	317.81	298.27	48927.52	5816.61	30713.08	6.74	0.128
3.5	316.48	297.54	59855.50	7907.80	31676.86	6.98	0.113
4	315.39	296.98	71396.35	10319.99	32591.43	7.19	0.102

Table 2. Results of wavy rectangular microchannel simulation

Inlet Velocity (m/s)	T_w (K)	T_f (K)	P_{inlet}	P_{outlet}	h at T_f	Nu	Friction factor (f)
0.5	346.45	324.09	4842.72	171.45	26831.27	5.51	0.4992
1	330.05	308.75	12349.45	666.44	28168.58	5.99	0.3121
1.5	323.47	303.60	21179.21	1487.81	30208.27	6.52	0.2338
2	319.41	301.00	31114.10	2632.44	32581.92	7.10	0.1902
2.5	316.49	299.41	42078.73	4097.86	35136.50	7.68	0.1623
3	314.23	298.35	54032.10	5877.64	37781.47	8.29	0.1429
3.5	312.43	297.59	66984.33	7965.78	40417.21	8.91	0.1287
4	310.99	297.02	80953.34	10359.69	42954.40	9.48	0.1179

3.2. Trapezoidal (0.075 mm base) cross-section

To investigate potential changes in heat transfer enhancement characteristics, the rectangular cross-section was modified to a trapezoidal geometry while maintaining a constant hydraulic diameter of 0.133 mm. This modification was achieved by reducing the bottom edge length from 1 mm to 0.75 mm and adjusting the top edge length accordingly (cross-sectional details are provided in the geometry description section). Using the same simulation parameters as those used for the rectangular channel, both straight and wavy trapezoidal configurations were evaluated. Although the overall heat transfer decreased due to the reduction in bottom edge length, as shown in Figure 7, the primary objective was to assess whether the transition from a straight to a wavy channel would exhibit a different heat transfer enhancement trend compared to the rectangular case. Tables 3 and 4 present detailed results of the analysis. From the Nu/Nu_0 versus Re plot in Figure 8, it can be observed that there is no significant change in the heat transfer enhancement pattern for the trapezoidal cross-section.

Table 3. Results of straight trapezoidal (0.075 mm base) microchannel simulation

Inlet Velocity (m/s)	T_w (K)	T_f (K)	P_{inlet}	P_{outlet}	h at T_f	Nu	Friction factor (f)
0.5	348.53	323.35	4798.90	169.19	24918.26	5.11	0.493
1	332.50	308.36	12056.38	656.93	25990.87	5.51	0.304
1.5	326.43	303.35	20381.47	1468.65	27179.82	5.85	0.224
2	322.95	300.82	29500.02	2601.79	28352.97	6.16	0.179
2.5	320.59	299.29	39328.30	4058.30	29465.98	6.42	0.150
3	318.83	298.27	49816.12	5837.53	30513.28	6.67	0.130
3.5	317.46	297.53	60940.20	7940.06	31497.32	6.92	0.115
4	316.33	296.98	72686.77	10368.04	32424.48	7.14	0.104

Table 4. Results of wavy trapezoidal (0.075 mm base) microchannel simulation

Inlet Velocity (m/s)	T_w (K)	T_f (K)	P_{inlet}	P_{outlet}	h at T_f	Nu	Friction factor (f)
0.5	347.807	323.736	4894.515	169.977	26066.915	5.35	0.504
1	331.136	308.586	1246.792	660.558	27825.508	5.90	0.315
1.5	324.396	303.500	2137.245	1475.739	30028.229	6.46	0.236
2	320.247	300.925	3137.203	2612.924	32473.581	7.06	0.192
2.5	317.271	299.362	4238.849	4067.637	35036.321	7.64	0.163
3	314.980	298.312	5438.943	5835.501	37645.724	8.24	0.144
3.5	313.156	297.560	6734.652	7909.449	40231.107	8.84	0.129
4	311.675	296.995	8128.118	10286.619	42741.781	9.41	0.118

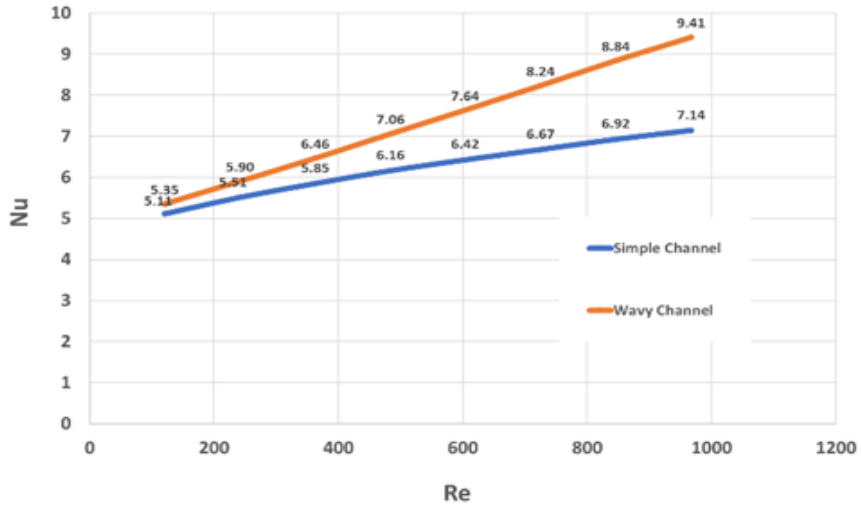

Figure 7. Comparison of Nusselt number in wavy and straight trapezoidal channel (0.075mm base) versus Re

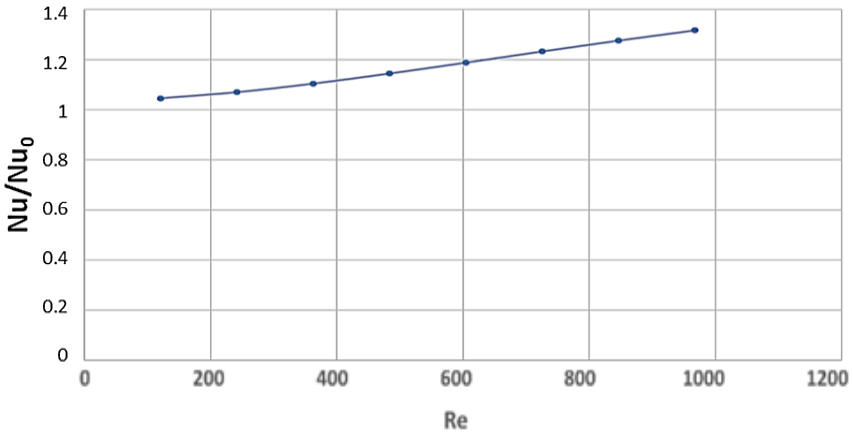

Figure 8. Comparison of Nu/Nu_0 versus Re for trapezoidal (0.075mm base) channel

3.3. Trapezoidal (0.055 mm base) cross-section

Previous observations demonstrated minimal variation in heat transfer enhancement when the MCHS configuration transitioned from a straight to a wavy profile. To further explore the influence of trapezoidal geometry on heat transfer performance while maintaining a constant hydraulic diameter, an alternative trapezoidal cross-section was considered. This modification involved reducing the bottom edge length to 0.055 mm and adjusting the top edge length accordingly to retain the same hydraulic diameter. The analytical results, presented in Tables 5 and 6, aligned with expectations—showing no significant improvement in heat transfer between the straight and wavy trapezoidal microchannels. These findings are illustrated in Figure 9. Furthermore, the Nu/Nu_0 versus Re plot in

Figure 10 confirms that the heat transfer enhancement trend closely resembles that of the previous two cases.

Table 5. Results of straight trapezoidal (0.055 mm base) microchannel simulation

Inlet Velocity (m/s)	T_w (K)	T_f (K)	P_{inlet}	P_{outlet}	h at T_f	Nu	Friction factor (f)
0.5	349.943	322.496	4745.789	170.999	23448.888	4.82	0.488
1	333.808	307.955	1190.497	662.539	24895.391	5.29	0.300
1.5	327.552	303.077	2013.712	1481.589	26296.307	5.66	0.221
2	323.932	300.617	2917.288	2625.768	27605.525	6.00	0.177
2.5	320.59	299.131	3892.187	4097.599	28810.501	6.28	0.148
3	319.641	298.134	4934.151	5896.754	29926.018	6.55	0.129
3.5	318.204	297.419	6040.776	8023.043	30963.995	6.81	0.114
4	317.033	296.880	7211.215	10478.391	31935.305	7.03	0.103

Table 6. Results of wavy trapezoidal (0.055 mm base) microchannel simulation

Inlet Velocity (m/s)	T_w (K)	T_f (K)	P_{inlet}	P_{outlet}	h at T_f	Nu	Friction factor (f)
0.5	349.1017	323.2936	4868.275	177.023	24938.06	5.12	0.500
1	332.3624	308.3987	1237.916	682.492	26857.39	5.70	0.312
1.5	325.4955	303.4059	2120.346	1520.382	29135.93	6.27	0.233
2	321.2258	300.8629	3111.374	2686.804	31606.5	6.87	0.189
2.5	318.1524	299.3092	4201.004	4176.030	34155.69	7.45	0.161
3	315.8274	298.2626	5384.813	5983.292	36641.65	8.02	0.142
3.5	314.0094	297.5125	6657.124	8099.100	39013.38	8.58	0.127
4	312.5441	296.6504	8020.204	10522.583	40494.06	8.92	0.116

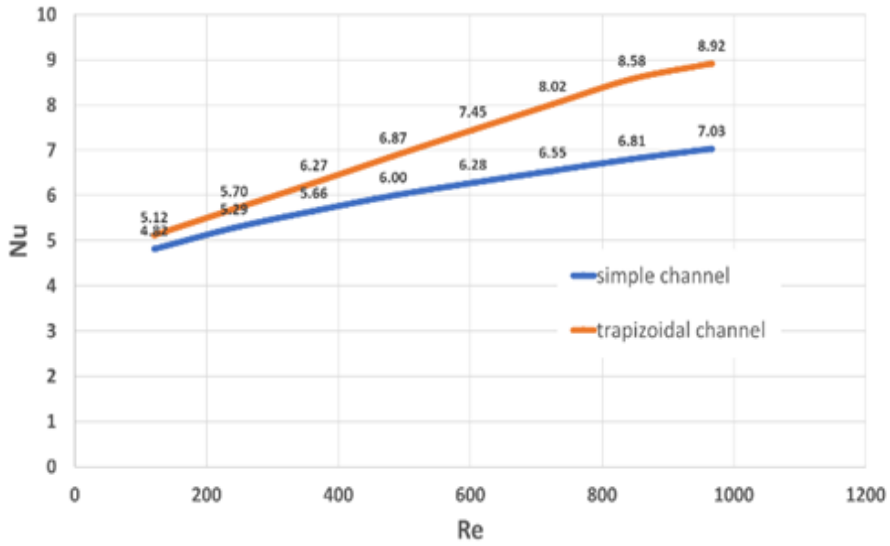

Figure 9. Comparison of Nusselt number in wavy and straight trapezoidal channel (0.055mm base) versus Re

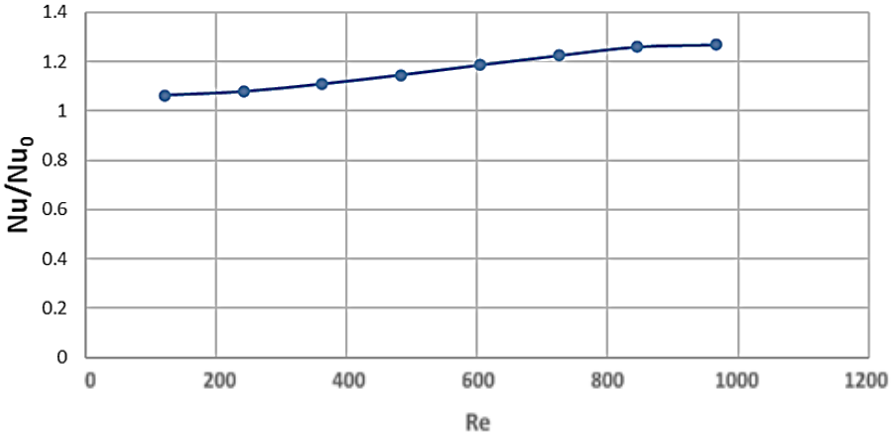

Figure 10. Comparison of Nu/Nu_0 versus Re for trapezoidal (0.055mm base) channel

3.4. Trapezoidal (0.18 mm top) cross-section

To evaluate the influence of hydraulic diameter on heat transfer enhancement during the transition from a straight to a wavy MCHS configuration, a distinct trapezoidal channel with a hydraulic diameter of 0.144 mm was introduced. The top width was maximized within the constraints of fitting both straight and wavy channel configurations within the limited width of a single MCHS unit. Detailed geometric specifications are provided in the geometry description section. The analytical results, presented in Tables 7 and 8, clearly indicate that variations in hydraulic diameter have no significant effect on the heat transfer enhancement pattern when transitioning from a straight to a wavy channel profile. Consistent with previous cases, heat transfer increases with rising inlet water velocity in both channel configurations. However, the enhancement becomes more pronounced with increasing Reynolds number when the geometry shifts from straight to wavy, as shown in Figure 11. Furthermore, the Nu/Nu_0 versus Re plot in Figure 12 closely resembles the trends observed in earlier cases, reinforcing the conclusion that hydraulic diameter does not significantly influence the heat transfer enhancement pattern in wavy microchannels.

Table 7. Results of straight trapezoidal (0.18 mm top) microchannel simulation

Inlet Velocity (m/s)	T_w (K)	T_f (K)	P_{inlet}	P_{outlet}	h at T_f	Nu	Friction factor (f)
0.5	348.4972	318.4165	4183.59	174.20	21037.03	4.67	0.462
1	333.6793	305.9161	10448.61	674.91	22793.15	5.23	0.281
1.5	327.6832	301.7112	17662.34	1505.95	24365.03	5.67	0.207
2	324.1465	299.588	25622.89	2666.01	25767.49	6.05	0.165
2.5	321.7166	298.3042	34270.57	4156.98	27028.86	6.37	0.139
3	319.8983	297.4429	43568.79	5979.04	28180.77	6.66	0.120
3.5	318.4631	296.8244	53495.23	8132.11	29244.34	6.95	0.107
4	317.2883	296.3584	64035.67	10616.09	30234.69	7.19	0.096

Table 8. Results of wavy trapezoidal (0.18 mm top) microchannel simulation

Inlet Velocity (m/s)	T_w (K)	T_f (K)	P_{inlet}	P_{outlet}	h at T_f	Nu	Friction factor (f)
0.5	347.8324	319.348	4402.334	186.68973	22216.00	4.93	0.486
1	332.527	306.2562	11292.53	716.170626	24087.94	5.52	0.305
1.5	325.5687	301.9826	19584.88	1585.84036	26829.76	6.24	0.230
2	321.6665	299.901	29146.65	2791.39119	29073.97	6.83	0.190
2.5	318.3624	298.6125	39924.29	4317.6392	32041.15	7.55	0.164
3	315.925	297.8054	51889.38	6155.82136	34924.03	8.26	0.146
3.5	313.967	296.964	64974.5	8287.02453	37217.52	8.84	0.133
4	312.389	296.106	79220.42	10705.8233	38863.20	9.25	0.123

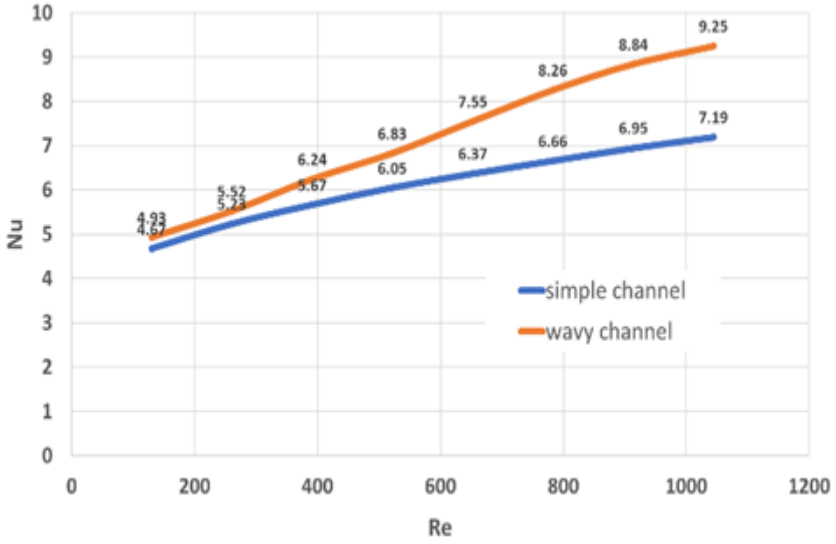

Figure 11. Comparison of Nusselt number in wavy and straight trapezoidal channel (0.18mm top) versus Re

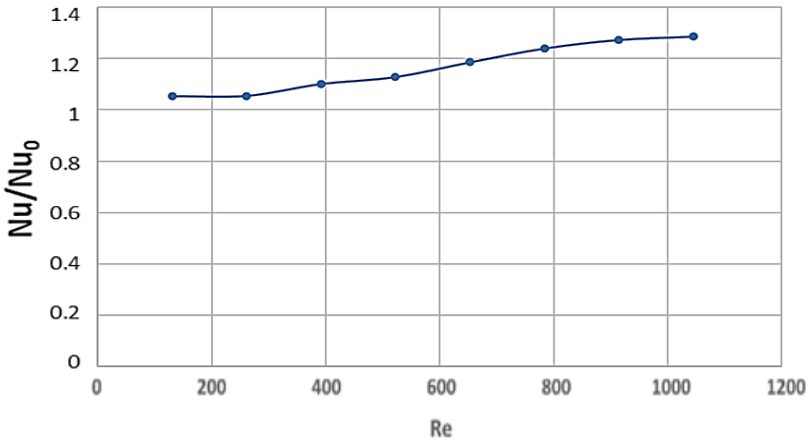

Figure 12. Comparison of Nu/Nu_0 versus Re for trapezoidal (0.18mm top) channel

3.5. Discussion

Based on the simulation results presented in Tables 1–8, a comparative analysis was conducted to identify the microchannel geometry that provides the best thermal performance in terms of the Nusselt number (Nu) and friction factor (f), as summarized in Table 9. These two parameters are key performance indicators: a higher Nusselt number signifies improved convective heat transfer [25], while a lower friction factor corresponds to reduced pressure drop and lower pumping power requirements [26].

At all inlet velocities, the wavy rectangular microchannel (Table 2) and the wavy trapezoidal microchannels (Tables 4, 6, and 8) consistently demonstrate higher Nusselt numbers compared to their straight counterparts. Among these, the wavy trapezoidal channel with a 0.18 mm top width (Table 8) achieved a maximum Nu of 9.25 at 4 m/s, while the wavy rectangular channel (Table 2) slightly outperformed it with a Nu of 9.48 at the same velocity. In terms of pressure drop, the straight rectangular microchannel (Table 1) recorded the lowest friction factor, f = 0.102 at 4 m/s, indicating excellent hydraulic efficiency. However, among the wavy geometries, the wavy trapezoidal channel with a 0.18 mm top width also exhibited a relatively low friction factor of f = 0.123 at 4 m/s, making it more favorable than the other wavy profiles.

These results suggest that the wavy rectangular microchannel delivers the highest overall heat transfer performance, making it suitable for applications requiring maximum thermal efficiency. Nevertheless, the wavy trapezoidal microchannel with a 0.18 mm top width offers the most favorable trade-off between enhanced heat transfer and moderate pressure drop. This makes it the most practical and efficient design for real-world applications where both thermal and hydraulic performance must be optimized. On the other hand, although the straight rectangular microchannel exhibits the

lowest pressure drop, it falls short in heat transfer enhancement, limiting its suitability for high power-density cooling scenarios.

Table 9. Comparison summary of various geometry performance trade-off

Geometry	Max. Nu	Min. f	Nu/f Ratio	Remarks
Wavy rectangular	9.48	0.1179	~80.4	Highest Nu, but slightly higher *f* than straight rectangular
Wavy Trapezoidal (0.18 mm top)	9.25	0.123	~75.2	Excellent balance of high Nu and low *f*
Straight rectangular	7.19	0.102	~70.5	Best in hydraulic efficiency but lower heat transfer
Other wavy trapezoidal	8.84–9.41	0.116–0.129	~70–78	Good performance but slightly more friction

4. Conclusions

This study presents a Computational Fluid Dynamics (CFD) analysis of laminar water flow and heat transfer in three-dimensional microchannels with both straight and wavy wall configurations, focusing on rectangular and trapezoidal cross-sections. Simulations were conducted under steady-state conditions, with constant bottom wall heat flux and conjugate boundary conditions. The results consistently show that introducing sinusoidal waviness along the channel walls significantly enhances heat transfer compared to straight channels, with only a modest increase in pressure drop. For all geometries examined, the Nusselt number (Nu) increased with Reynolds number (Re), indicating improved convective heat transfer at higher flow rates. However, the rate of increase was notably higher in wavy microchannels than in their straight counterparts. Quantitatively, at an inlet velocity of 4 m/s, the wavy rectangular microchannel achieved a maximum Nusselt number of 9.48, compared to 7.19 for the straight rectangular channel, representing an enhancement of approximately 32%. Similarly, for the wavy trapezoidal microchannel with a top width of 0.18 mm, the Nusselt number reached 9.25, compared to 7.19 in the straight case—indicating a 29% improvement. The Nu/Nu_0 versus Re plots for all geometries showed a similar upward trend, confirming that the enhancement in heat transfer due to wall waviness is consistent across different channel shapes. Importantly, when the hydraulic diameter was kept constant, changing the cross-sectional shape from rectangular to trapezoidal had a negligible effect on the heat transfer enhancement trend. This implies that the primary driver of improvement is the introduction of wall waviness, not the specific cross-sectional geometry, provided the hydraulic diameter remains unchanged. Overall, this study confirms that wavy microchannels significantly improve thermal performance without incurring excessive pressure loss. These findings are valuable for the design of compact and efficient microchannel heat sinks for high-performance electronic cooling applications.

Nomenclature

Symbol	Description	Unit
A	Area	m^2
C_p	Specific heat	$J\ kg^{-1}K^{-1}$
H	Heat transfer coefficient	$W\ m^{-2}\ K^{-1}$
Nu	Nusselt number	-
Re	Reynolds number	-
h	Enthalpy	j/kgmol
K	Thermal conductivity of fluid	j/s m K
T	Temperature	^oC
T_w	Temp of the bottom wall	^oC
T_f	Temp of the flowing water	^oC
D	Hydraulic mean diameter of channel	mm
Q	Total Heat transfer	W/m^2
L_c	Overall length of the microchannel	mm
m	Mass flow rate of water	$kg\ s^{-1}$
f	Friction factor	-

x, y, z	Three coordinates	
S	Volumetric heat source	J/m^3
W_c	Width of the channel	mm
H_c	Height of the channel	mm
P_{inlet}	Inlet pressure	Pa
P_{outlet}	Outlet pressure	Pa

References

[1] Y. Sui, C. J. Teo, P. S. Lee, Y. T. Chew, and C. Shu, "Fluid flow and heat transfer in wavy microchannels," *Int J Heat Mass Transf*, vol. 53, no. 13–14, pp. 2760–2772, Jun. 2010, doi: 10.1016/j.ijheatmasstransfer.2010.02.022.

[2] IEEE IRDS, "International roadmap for devices and systems: 2021," 2021. Accessed: Jan. 01, 2025. [Online]. Available: https://irds.ieee.org/images/files/pdf/2021/2021IRDS_ES.pdf

[3] A. Datta, D. Debbarma, N. Biswas, D. Sanyal, and A. K. Das, "The role of flow structures on the thermal performance of microchannels with wall features," *J Therm Sci Eng Appl*, vol. 13, no. 2, Apr. 2021, doi: 10.1115/1.4047709.

[4] D. B. Tuckerman and R. F. W. Pease, "High-performance heat sinking for VLSI," *IEEE Electron Device Letters*, vol. 2, no. 5, pp. 126–129, May 1981, doi: 10.1109/EDL.1981.25367.

[5] W. Qu and I. Mudawar, "Experimental and numerical study of pressure drop and heat transfer in a single-phase micro-channel heat sink," *Int J Heat Mass Transf*, vol. 45, no. 12, pp. 2549–2565, Jun. 2002, doi: 10.1016/S0017-9310(01)00337-4.

[6] H. Y. Wu and P. Cheng, "An experimental study of convective heat transfer in silicon microchannels with different surface conditions," *Int J Heat Mass Transf*, vol. 46, no. 14, pp. 2547–2556, Jul. 2003, doi: 10.1016/S0017-9310(03)00035-8.

[7] K. C. Toh, X. Y. Chen, and J. C. Chai, "Numerical computation of fluid flow and heat transfer in microchannels," *Int J Heat Mass Transf*, vol. 45, no. 26, pp. 5133–5141, Dec. 2002, doi: 10.1016/S0017-9310(02)00223-5.

[8] G. Gamrat, M. Favre-Marinet, and D. Asendrych, "Conduction and entrance effects on laminar liquid flow and heat transfer in rectangular microchannels," *Int J Heat Mass Transf*, vol. 48, no. 14, pp. 2943–2954, Jul. 2005, doi: 10.1016/j.ijheatmasstransfer.2004.10.006.

[9] M. K. Kang, J. H. Shin, H.-H. Lee, and K. Chun, "Analysis of laminar convective heat transfer in micro heat exchanger for stacked multi-chip module," *Microsystem Technologies*, vol. 11, no. 11, pp. 1176–1186, Oct. 2005, doi: 10.1007/s00542-005-0590-9.

[10] P.-S. Lee, S. V. Garimella, and D. Liu, "Investigation of heat transfer in rectangular microchannels," *Int J Heat Mass Transf*, vol. 48, no. 9, pp. 1688–1704, Apr. 2005, doi: 10.1016/j.ijheatmasstransfer.2004.11.019.

[11] V. K. Pandey, V. Choudhary, C. Ranganayakulu, and A. A. M., "Thermal hydraulic performance and characteristics of a microchannel heat exchanger: Experimental and numerical investigations," *ASME Journal of Heat and Mass Transfer*, vol. 147, no. 2, Feb. 2025, doi: 10.1115/1.4067012.

[12] M. N. Akram, K. Mohiuddin, M. A. S. Akash, F. Ibeh, and M. S. Kibria, "Numerical investigation on enhanced thermal performance of rectangular microchannels with triangular ribs," *Archives of Advanced Engineering Science*, pp. 1–11, Sep. 2024, doi: 10.47852/bonviewAAES42023989.

[13] T. Yu, X. Guo, and Y. Tang, "Numerical investigations of heat transfer augmentation in a microchannel heat sink with different shaped periodic reentrant cavities on channel sidewalls," *Can J Phys*, vol. 102, no. 11, pp. 590–603, Nov. 2024, doi: 10.1139/cjp-2023-0275.

[14] D. K. Raj, A. Datta, and N. K. Soni, "Design of the microchannels heat sink to augment the thermal performance using different type of cavity with or without wavy channel," *Heat Transfer Engineering*, vol. 46, no. 4–5, pp. 432–449, Mar. 2025, doi: 10.1080/01457632.2024.2317605.

[15] Q. Wang, J. Tao, Z. Cui, T. Zhang, and G. Chen, "Passive enhanced heat transfer, hotspot management and temperature uniformity enhancement of electronic devices by micro heat sinks: A review," *Int J Heat Fluid Flow*, vol. 107, p. 109368, Jul. 2024, doi: 10.1016/j.ijheatfluidflow.2024.109368.

[16] M. A. Wazir, K. Akhtar, U. Ghani, M. Wajib, S. Shaukat, and H. Ali, "Thermal enhancement of microchannel heat sink using pin-fin configurations and geometric optimization," *Engineering Research Express*, vol. 6, no. 1, p. 015526, Mar. 2024, doi: 10.1088/2631-8695/ad3400.

[17] S. Ahmed Memon, S. Akhtar, T. Ahmad Cheema, and C. Woo Park, "Enhancing heat transfer in microchannels: A systematic evaluation of crescent-like fin and wall geometries with secondary flow," *Appl Therm Eng*, vol. 239, p. 122099, Feb. 2024, doi: 10.1016/j.applthermaleng.2023.122099.

[18] Yew Wai Loon, Nor Azwadi Che Sidik, and Yutaka Asako, "Numerical analysis of fluid flow and heat transfer characteristics of novel microchannel heat sink," *Journal of Advanced Research in Numerical Heat Transfer*, vol. 15, no. 1, pp. 1–23, Jan. 2024, doi: 10.37934/arnht.15.1.123.

[19] W. Qu and I. Mudawar, "Experimental and numerical study of pressure drop and heat transfer in a single-phase micro-channel heat sink," *Int J Heat Mass Transf*, vol. 45, no. 12, pp. 2549–2565, Jun. 2002, doi: 10.1016/S0017-9310(01)00337-4.

[20] G. Xia, Y. Zhai, and Z. Cui, "Numerical investigation of thermal enhancement in a micro heat sink with fan-shaped reentrant cavities and internal ribs," *Appl Therm Eng*, vol. 58, no. 1–2, pp. 52–60, Sep. 2013, doi: 10.1016/j.applthermaleng.2013.04.005.

[21] I. A. Ghani, N. Kamaruzaman, and N. A. C. Sidik, "Heat transfer augmentation in a microchannel heat sink with sinusoidal cavities and rectangular ribs," *Int J Heat Mass Transf*, vol. 108, pp. 1969–1981, May 2017, doi: 10.1016/j.ijheatmasstransfer.2017.01.046.

[22] Y. F. Li, G. D. Xia, D. D. Ma, Y. T. Jia, and J. Wang, "Characteristics of laminar flow and heat transfer in microchannel heat sink with triangular cavities and rectangular ribs," *Int J Heat Mass Transf*, vol. 98, pp. 17–28, Jul. 2016, doi: 10.1016/j.ijheatmasstransfer.2016.03.022.

[23] G. Xia, L. Chai, H. Wang, M. Zhou, and Z. Cui, "Optimum thermal design of microchannel heat sink with triangular reentrant cavities," *Appl Therm Eng*, vol. 31, no. 6–7, pp. 1208–1219, May 2011, doi: 10.1016/j.applthermaleng.2010.12.022.

[24] G. Xia, L. Chai, M. Zhou, and H. Wang, "Effects of structural parameters on fluid flow and heat transfer in a microchannel with aligned fan-shaped reentrant cavities," *International Journal of Thermal Sciences*, vol. 50, no. 3, pp. 411–419, Mar. 2011, doi: 10.1016/j.ijthermalsci.2010.08.009.

[25] C. B. Rocha, N. C. Constantinou, and S. G. L. Smith, "The Nusselt numbers of horizontal convection," *J. Fluid Mech.*, vol. 894, p. A24, 2020, doi: 10.1017/jfm.2020.269.

[26] S. Saito, S. Baba, K. Kinoshita, and N. Takada, "Thermal-hydraulic performance of additively manufactured AlSi10Mg crossflow minichannel heat exchangers," *SSRN*, 2024, doi: 10.2139/ssrn.5039654.